Monthly Notices
of the
ROYAL ASTRONOMICAL SOCIETY

MNRAS **429,** 2894–2902 (2013) doi:10.1093/mnras/sts471

An improved model for the infrared emission from the zodiacal dust cloud: cometary, asteroidal and interstellar dust

M. Rowan-Robinson★ and B. May

Astrophysics Group, Blackett Laboratory, Imperial College of Science Technology and Medicine, Prince Consort Road, London SW7 2AZ

Accepted 2012 November 21. Received 2012 November 19; in original form 2012 October 5

ABSTRACT

We model the infrared emission from zodiacal dust detected by the *IRAS* and *COBE* missions, with the aim of estimating the relative contributions of asteroidal, cometary and interstellar dust to the zodiacal cloud. Our most important result is the detection of an isotropic component of foreground radiation due to the interstellar dust.

The dust in the inner Solar system is known to have a fan-like distribution. If this is assumed to extend to the orbit of Mars, we find that cometary, asteroidal and interstellar dust account for 70, 22 and 7.5 per cent of the dust in the fan. We find a worse fit if the fan is assumed to extend to the orbit of Jupiter. Our model is broadly consistent with the analysis of interplanetary dust detected by Ulysses and other spacecraft. Our estimate of the mass–density of interstellar dust in the inner Solar system is consistent with estimates from Ulysses at 1.5 au, but is an order of magnitude higher than Ulysses estimates at $r > 4$ au. Only 1 per cent of the zodiacal dust arriving at the earth would be interstellar, in our model.

Our models can be further tested by ground-based kinematical studies of the zodiacal cloud, which need to extend over a period of years to monitor solar cycle variations in interstellar dust, by dynamical simulations, and by in situ measurements from spacecraft.

Key words: zodiacal dust – interplanetary medium – planetary systems.

1 INTRODUCTION

The zodiacal dust is an important constituent of the Sun's debris disc, and contains clues to the recent history of that disc. In this paper, we attempt to estimate the relative contributions of asteroidal, cometary and interstellar dust to the infrared emission from zodiacal dust detected by *IRAS* and *COBE*. This is the first attempt to model the data from both missions simultaneously.

1.1 Pre-*IRAS*

Early work on modelling scattered optical zodiacal light was extensively reviewed by Giese et al. (1985), Giese, Kneissel & Rittich (1986) and Leinert (1985). The consensus from these studies was that the number density of dust grains in the inner Solar system followed a distribution

$$n(r) = n_0 r^{-\gamma} f(\beta_0), \quad (1)$$

where r is the distance from the Sun in au and β_0 is the elevation from the symmetry plane of the dust, with $\gamma \sim 1.3$.

A popular form for $f(\beta_0)$ was the 'fan' distribution

$$f(\beta_0) = \exp - P|\sin\beta_0|. \quad (2)$$

1.2 Kinematical studies

Early work on the kinematics of the zodiacal dust was begun by the Imperial group in the late 1960s (Reay & Ring 1968; Hicks, May & Reay 1974; East & Reay 1984). Hicks et al. (1972, 1974) raised the possibility that some of the zodiacal dust in the vicinity of earth may be of interstellar origin, an idea that was developed more fully by May (2007). May's estimate was that the kinematic asymmetry seen by Hicks et al. (1974) between 1971 September–October and 1972 April could be explained if ∼10 per cent of the dust were part of a linear flow, due for example to interstellar dust, with the rest being due to dust in circular orbits, arising from cometary and asteroidal sources.

More recent kinematic measurements of zodiacal dust have been made by Reynolds, Madsen & Moseley (2004), using the Wisconson H-alpha Machine (WHAM) spectrometer, and these observations have been modelled by Madsen et al. (2006) using models of cometary and asteroidal dust published by Ipatov et al. (2006). However May (2007) still found that there was a discrepancy between the observations of Reynolds et al. (2004) and those of East & Reay (1984), which might still leave room for a seasonal variation in zodiacal dust kinematics due to the presence of interstellar dust.

1.3 *IRAS*

Our understanding of the zodiacal dust was transformed by the *IRAS* mission in 1983, which gave the first all-sky maps of the

★E-mail: mrr@imperial.ac.uk

zodiacal dust emission and discovered both the *IRAS* Zodiacal Bands, attributed to collisions between members of asteroid families (Dermott et al. 1984; Low et al. 1984; Sykes & Greenberg 1986; Sykes 1990; Grogan, Dermott & Xu 2001), of which at least five are now known, contributing about 10 per cent of the total zodiacal emission in the infrared, and, on a small scale, cometary dust trails (Sykes et al. 1986). These demonstrated that both collisions between asteroids and comet debris must, at some level, contribute to the zodiacal dust cloud. *IRAS* also revealed a local ring of dust near the Earth (Dermott et al. 1994; Leisawitz et al. 1994; Reach et al. 1995).

The first full models of infrared emission from the zodiacal dust cloud were given by Rowan-Robinson et al. (1990, 1991) and Jones & Rowan-Robinson (1993). The novel features of these models were as follows.

(i) Use of a modified fan distribution

$$f(\beta_0) = (\cos\beta_0)^Q \exp - P\sin|\beta_0|^\xi . \quad (3)$$

This incorporates the $(cos\beta_0)^Q$ term introduced by Murdock & Price (1985) and the smoothing at the symmetry plane introduced by Deul & Wostencroft (1988), where

$$\xi = 2 - |z/z_0|, \quad \text{for} \quad |z| < z_0, = 1 \text{ otherwise},$$

and $z_0 = 0.065$ au.

Dust grains were assumed to be grey ($Q_\nu = 1$) at 12–100 μm, so their typical radii needed to be $> 10\mu$m.

(ii) Detailed models of the two strongest pairs of narrow asteroid band features at $|\beta = 1\overset{\circ}{.}4$ and $10\overset{\circ}{.}2$.

(iii) Identification of an additional component of broad asteroidal bands centred at $|\beta| \sim 10^\circ$. Rowan-Robinson et al. (1991) suggested that the cooler spectral energy distribution of the broad-bands pointed to a distant origin for these bands, perhaps at ∼50 au, but a parallax test performed by Jones & Rowan-Robinson (1993) using the third *IRAS* HCON showed that they are consistent with being, like the narrow bands, at $r \sim 1.5$–3 au. Jones & Rowan-Robinson's (1993) fan model extended to $r = 1.5$ au and they found that asteroidal dust could account for ∼25 per cent of the dust involved in the fan component. So a major deficiency of that model is to account for the remaining ∼75 per cent of the dust in the fan.

Liou, Dermott & Xu (1995) used a dynamical analysis fitted to the *IRAS* data to conclude that 74 per cent of the zodiacal cloud was of cometary origin, while 26 per cent was asteroidal. Durda & Dermott (1997) concluded that as much as 34 per cent could be asteroidal.

Nesvorny et al. (2010) have modelled the dynamics of cometary dust and compared results with *IRAS* data, concluding that over 90 per cent of zodiacal dust is cometary. However, their use of smoothed data means that the narrow asteroidal bands are smoothed out and it is likely that they have underestimated the contribution of asteroidal dust.

1.4 Ulysses

The next major contribution to understanding of the nature and origin of zodiacal dust was in situ measurements of zodiacal dust by Ulysses (1990–2009) and other spacecraft. Divine (1993) analysed Ulysses and other data to identify five different components of interstellar dust. The three dominant components are the core (fan) component, extending to ∼2 au, an asteroidal component dominating from 1–3 au and a relatively isotropic halo component which becomes significant at ∼3 au and dominates at large distances (see also the review of Solar system dust by Grun et al. 1993).

One of the major discoveries of Ulysses was the strong role of interstellar dust in the Solar system, especially at greater distances from the Sun (see the review by Mann 2010). Interstellar dust has also been detected in the Solar system by the Galileo, Cassini and Stardust spacecraft (Altobelli et al. 2003; Grun et al. 2005; Kruger et al. 2010; Mann 2010; Sterken et al. 2012a). The density of interstellar dust in the Solar system varies with time, with a strong dependence on the solar cycle. Because the dust particles become charged, their motion is strongly influenced by the plasma flow, and the Earth's bow shock excludes much of the dust, especially the smaller particles. At times of solar maximum, magnetic field reversals mean that interstellar dust is allowed into the inner Solar system. Its relatively high velocity relative to the Sun, typically $\sim 26\,\mathrm{km\,s^{-1}}$, means that this dust can traverse the ∼200 au from the magnetopause in ∼50 yr. By contrast dust in approximately circular orbit around the sun, and spiralling inwards under the influence of the Poynting–Robertson effect, takes ∼10 000 yr to travel from the asteroid belt to the Earth (Gustafsen, Misconi & Rusk 1987).

Interstellar dust within a cylindrical column with the Hoyle–Lyttleton radius $2GM_\odot/v_\odot^2 \sim 4$ au (Hoyle & Lyttleton 1939) would be gravitationally trapped by the Sun and can in principle be an important supply source for the zodiacal dust cloud. Since the time-scale for this gravitational trapping is of the order of ∼2 yr, the quantity of interstellar dust in the inner Solar system may vary on a time-scale of years, and would certainly be expected to vary over the solar cycle. Interstellar dust with impact parameter appreciably greater than 4 au would pass through the inner Solar system rapidly but may still contribute to the infrared emission detected by *IRAS* and Diffuse Infrared Background Experiment (DIRBE).

The planets have a negligible effect on the motion of the interstellar dust. By contrast the very slow passage of dust grains spiralling inwards under the Poynting–Robertson effect ensures that each planet can significantly modify the orbits of dust grains and the vertical distribution of dust density.

Grogan, Dermott & Gustafson (1996) simulated the flow of interstellar dust into the inner Solar system, including the effects of gravity, radiation pressure and magnetic forces on the dust grains. They found that the distribution of this dust tends to be approximately isotropic over most of the sky, with a column downstream of the flow direction in which larger grains ($\gg 0.3$ μm) are focused by the Hoyle–Lyttleton accretion, and from which smaller grains (<0.3 μm) are excluded by the combined effects of radiation pressure and magnetic forces. They concluded that the contribution of local interstellar grains to the infrared foreground would be small ($<0.1\,\mathrm{MJy\,sr^{-1}}$ at 12 μm), but this was based on rather a low estimate of the density of interstellar dust at 5 au (see Section 6 below). A more detailed simulation of the flow of interstellar dust through the Solar system, under the action of gravity, radiation pressure and Lorentz forces, through the different phases of the solar cycle, has been given by Sterken et al. (2012b). They find strong variation with time of the density of interstellar dust in the inner Solar system. They also find some systematic deviation from isotropy with time during the solar cycle, but this is unlikely to be detectable in the type of modelling we are carrying out here.

1.5 *COBE*

The DIRBE instrument on *COBE* mapped the zodiacal emission in 1989–90 with a different scan strategy to *IRAS*. Whereas *IRAS*

scanned from ecliptic pole to pole, the *COBE* spacecraft executed an additional circular motion which resulted in sampling the zodiacal emission at a wide range of solar elongations every day. A further advantage was that DIRBE, unlike *IRAS*, had an absolute calibration. The *IRAS* zodiacal measurements had a somewhat better resolution than DIRBE, and coupled with the fact that scans were at approximately constant solar elongation, this meant that *IRAS* gives better resolution of the fine structure in the zodiacal bands.

Kelsall et al. (1998) modelled the zodiacal emission detected by DIRBE using a slightly different modified exponential fan to Jones & Rowan-Robinson (JRR) with

$$f(\beta_0) = \exp -P(\sin|\beta_0| - z_0/2)^{\gamma_1}, \quad \text{for} \quad \sin|\beta_0| < z_0,$$
$$= \exp -P(\sin^2|\beta_0|/2z_0)^{\gamma_1}, \quad \text{for} \quad \sin|\beta_0| > z_0,$$

where $z_0 = 0.189$, $\gamma_1 = 0.942$.

No attempt was made to account for cometary or interstellar dust, but the fan is assumed to extend to 5.2 au. Their main innovation is inclusion of the ring of dust at $r \sim 1$ au and the blob trailing behind Earth, which had been first detected by Dermott et al. (1994) in the *IRAS* data, and confirmed by Reach et al. (1995). They justified the neglect of interstellar dust based on the work of Grogan et al. (1996).

In this paper, we revisit models for the combined *IRAS* and DIRBE observations of zodiacal dust, with a view to trying to determine the relative contributions of asteroidal, cometary and interstellar dust. The *IRAS* Zodiacal History File remains a key data set if full sampling of the asteroidal component is required. The DIRBE data, with its absolute calibration, are essential if an isotropic component like interstellar dust is to be detected. The components in our model are physically motivated, occupy distinct regions of the Solar system, and have different radial dependences. While dynamical simulations are essential for understanding the evolution of zodiacal dust, our approach provides a valid independent perspective.

2 INGREDIENTS OF THE MODEL

We aim to be strongly guided by the evidence from direct detection of interplanetary dust. We can expect major transformation of the vertical dust profile as each planetary orbit is crossed and so for our purposes we must allow for significant changes at the orbit of Mars, $r = 1.53$ au, and at the orbit of Jupiter, $r = 5.2$ au.

The main ingredients of the JRR (1993) model, the modified fan and asteroid bands, correspond well to two of the main components detected in spacecraft data. Their assumption that the fan terminates at $r = 1.5$ au is consistent with the Divine (1993) analysis, though we will explore here the possibility that it extends further. The radial dependence for the fan assumed by JRR was $r^{-1.0}$, guided by the expected behaviour of grains subject to the Poynting–Robertson effect, but the evidence for a radial dependence of $r^{-1.3}$ within 1.5 au now seems very strong and we use that dependence here. We initially use the JRR parameters for the asteroid bands, but will consider the possibility that the amplitudes need modification, to take account of the other ingredients used here. We will also look briefly at the possibility that the broad-bands extend to a greater distance than 3.1 au.

The first ingredient not incorporated by JRR, but included by Kelsall et al. (1998), is the solar ring and trailing blob and we have used the formalism of Kelsall et al. (1998) for these, but allowing the amplitudes to be a free parameter.

Secondly, we want to include a component corresponding to cometary dust. The dominant contribution is expected to be from Jupiter-family comets, which tend to have inclinations $<30^\circ$, have aphelia ranging from 5 to 30 au, and have their origin in the Kuiper belt. For the cometary contribution to the asteroidal dust we therefore expect a flattened distribution, but perhaps not so strongly flattened as the inner fan. We assume an exponential fan extending from $r = 1.5$ to 30 au, with exponent PCOM (to be determined), and assuming an r^{-1} radial distribution. Nesvorny et al. (2010) estimate that the contribution of Oort cloud comets is negligible and we were also not able to detect such a component.

Finally, for interstellar dust we assume an isotropic distribution, with uniform density, extending from $r = 0$ to 30 au. In reality the distribution of interstellar dust will be more complex, especially for larger and smaller grains (Sterken et al. 2012b), but isotropy is a reasonable first-order assumption in this attempt to detect interstellar dust through its infrared emission.

We assume that the cometary and interstellar components together contribute the 'halo' population identified by Divine (1993). The crucial distinction between the components in the model lies in their radial distribution, with asteroidal dust originating between 1.5 and 3.1 au, cometary dust extending from 1.5 au out to large distances, and interstellar dust extending through the whole Solar system. The fan is assumed to be supplied by the cometary and asteroidal components and extends to 1.5 au. So the components are quite distinct in their contribution to the infrared emission.

3 FITS TO *IRAS* DATA

The data we have used are version 3.0 of the *IRAS* Zodiacal History File, which lists position on the sky, UTCS and fluxes averaged over 0.5 degree^2 in the four *IRAS* bands. From this information the solar longitude can be calculated. Data heavily affected by cirrus are excluded, using a standard mask. The fan is assumed to have a symmetry plane specified by (Ω, i). We have not corrected for the relatively small effect of the Sun's displacement from the symmetry plane of the zodiacal dust cloud. The density of the dust in the fan is specified by equations (1) and (3). The dust grains are assumed to be large and grey, with a temperature dependence $T_1 r^{-0.5}$, with $T_1 = 255$ K. Variation of the temperature at 1 au, T_1, was explored but not found to improve the fits. The fan was assumed to extend out to a radius RMAX, initially taken to be 1.53 au.

The density of dust in the narrow bands was assumed to satisfy equation (1), with $\gamma = 1.0$ and

$$f_{nb}(\beta_0) = \exp G(|\beta_0| - \beta_{nb}), |\beta_0| < \beta_{nb}. \quad (4)$$

β_b was taken to be 1°.42 for the inner bands, corresponding to the Themis asteroid family. For the outer bands, JRR assumed $\beta_b = 10°.14$, corresponding to the Eos family, but Grogan et al. (2001) have shown that there is better agreement with the Veritas family, with $\beta_b = 9°.35$, and we confirm here that this gives a better fit to the *IRAS* data. The bands are assumed to extend from $r = 1.53$ to 3.1 au.

For the broad-bands identified by Rowan-Robinson et al. (1991) and modelled by JRR, we assume that they have their own symmetry plane characterized by (Ω_{bb}, i_{bb}). Their density is also assumed to be of the form of equation (1), with $\gamma = 1.0$ and

$$f_{bb}(\beta_1) = \exp\left[-(\beta_1 - \beta_{bb})^2/2\sigma_{bb}^2\right] + \exp\left[-(\beta_1 + \beta_{bb})^2/2\sigma_{bb}^2\right], \quad (5)$$

where β_{bb} is the latitude of the peaks above the symmetry plane and σ_{bb} is the peak width. These bands are assumed to extend from $r =$ 1.53 au to R2BF, where R2BF is normally taken to be 3.1 au, but the possibility of extension to greater distance is considered below. The grains in the broad-bands were also assumed to be large and we did not confirm the suggestion of JRR that the fits are improved if the broad-band grains are assumed to be small.

For cometary dust we assume a density dependence of the form equations (1) and (2), with $\gamma = 1.0$. We are assuming that cometary dust has a flattened distribution, but not as strongly flattened as the main zodiacal fan. Cometary dust is assumed to extend from $r =$ 1.53 to 30 au.

For interstellar dust we assume an isotropic and uniform distribution, extending from $r = 0$ to 30 au, based on the simulations of Grogan et al. (1996). We discuss below the expected departure from isotropy in a cone downstream of the Sun. The outer cutoff for cometary and interstellar dust, corresponding to the inner edge of the Kuiper belt, is arbitrary, and the fit to the *IRAS* data is not sensitive to this parameter. The Grogan et al. (1996) estimate of a negligible contribution by interstellar dust to the infrared foreground was based on a rather low density of interstellar dust, 2×10^{-27} gm cm^{-3}, at 5 au. Kimura, Mann & Jessberger (2003) and Mann (2010) report estimates 2–20 times higher than this and we believe it is worth allowing the density of interstellar dust to be a free parameter and see whether the resulting implied densities are unreasonable.

The interstellar dust grains can be expected to be smaller than those of cometary and asteroidal origin, and are indeed found to be so in the spacecraft studies (e.g. Grun et al. 1993). Our best solution was found to be with $Q_\nu \propto \nu$ for $\lambda > 24$ μm, $= 1$ for $\lambda \leq$ 24 μm, corresponding to grain radius ∼2–4 μm. The corresponding temperature distribution for these smaller grains was taken to be $T = 305\, r^{-0.4}$ K.

Finally, the ∼1 au ring and trailing blob are modelled using the formalism of Kelsall et al. (1998), but we allow the amplitudes to be a free parameter.

We estimated the rms fluctuation in each band at $|b| > 40^\circ$, $|\beta| > 20^\circ$ (after subtraction of the fan contribution) to be $\sigma_\nu = 0.42$, 0.55, 0.45 and 1.10 MJy sr^{-1} at 12, 25, 60 and 100 μm, respectively. We then minimize $\chi^2 = \Sigma[I_{\nu,IRAS} - C_\nu \int n(r, \lambda, \beta) B_\nu(T(r))\mathrm{d}s + D_\nu]^2/\sigma_\nu^2$. Because *IRAS* did not have an absolute calibration there is uncertainty in the zero-point in each band, with a quoted rms 0.66, 0.73, 0.38 and 1.19 MJy sr^{-1} at 12, 25, 60 and 100 μm. This makes the estimation of any isotropic component like our assumed interstellar component problematical.

The approach we have followed here, is to use the offsets D_ν estimated for the *IRAS* data by the DIRBE team from direct comparison of DIRBE and *IRAS* data. These are given as −0.48, −1.32, 0.13 and −1.47 MJy sr^{-1} at 12, 25, 60 and 100 μm (Beichman & Wheelock 1993, *IRAS* project note, www.ipac.caltech.edu/ipac/newsletters/oct93/cobe.html). We then minimize the total χ^2, summed over the four *IRAS* bands, allowing a free calibration factor C_ν.

Any isotropic component has to be consistent with the limits on an isotropic component set by DIRBE, which are given as (2σ) 1.9, 4.2, 1.5 and 1.3 MJy sr^{-1} at 12, 25, 60 and 100 μm (Hauser et al. 1998) (see Section 5).

We find that both cometary and interstellar dust components were positively detected, in that the fit improved significantly when they were included. This is consistent with the results of direct detection of interstellar dust by Ulysses and other spacecraft (Grun et al. 1993).

4 RESULTS OF FITS TO *IRAS* DATA ALONE

The results of varying the parameters of the model are shown in Table 1, with the penultimate column showing the sum of the reduced χ^2 summed over the four *IRAS* bands. The first line corresponds to the preferred model of JRR (1993), with their parameters for the narrow and broad-bands. The second line shows the effect of changing the radial density index to $\gamma = 1.3$.

We now add in the ring and trailing blob, cometary and interstellar components, tune the amplitudes of these, and then solve again for the parameters of the fan, Q and P. The fit to the *IRAS* data is significantly improved. We then make a number of small adjustments to the model which improve the fit: (i) we assumed that the outer narrow bands are due to the Veritas family, with $\beta_{nb} = 9.^\circ35$ and adjusted G2 to 0.12; (ii) we tuned the parameters for the symmetry plane of the broad-bands and found a better fit at $\Omega_{bb} = 110^\circ$, $i_{bb} = 2.^\circ6$; (iv) we tuned the parameters for the symmetry plane of the fan and found $\Omega = 78^\circ$, $i = 1.^\circ50$. A multiparameter grid-search fitted to the *IRAS* data with parameters P, Q, z0, AMPBB, COM1, for different values of ISD1, yielded uncertainties of 2 per cent for P, Q, and 10 per cent for other parameters. We estimate the uncertainty in ISD1 as 20 per cent. The best-fitting parameters are shown in line 3 of Table 1, shown in bold, model A.

Fig. 1 shows latitude profiles in the four *IRAS* bands for a scan with solar longitude $90.^\circ61$, compared with the predictions of model A. The fit is excellent. Figs 2 and 3 show latitude profiles at 25 μm for scans spread throughout the survey, after subtraction of the fan component, compared with the predictions of the other ingredients of the model. The fits are spectacularly good. The adjustments to the parameters of the narrow (asteroidal) and broad-bands, and the inclusion of components corresponding to cometary and interstellar dust, all contribute to the improvement of the fits compared with the work of JRR. We found the amplitude of the trailing blob needed to be smaller than that assumed by Kelsall et al. (1998).

For our basic model A, with the fan extending to 1.53 au, the asteroidal dust in the narrow and broad-bands, cometary dust and interstellar dust, integrated over all ecliptic latitudes, contribute 22.2, 70.4 and 7.5 per cent, respectively, of the density of dust, relative to the fan. The total contribution from the three components adds to exactly 100 per cent of the density in the fan (this was not

Table 1. Parameters for new zodiacal dust models.

Fan Q	P	z0	RMAX	Narrow AMP1	Bands AMP2	Broad b. AMPBB	Ring AMPSR	Blob AMPBL	Comet COM1	PCOM	I.S.D. ISD1	χ^2_n *IRAS*	DIRBE
8.0	2.85	0.065	1.52	0.030	0.039	0.029	–	–	–	–	–	5.03	($\gamma = 1.0$)
8.0	2.85	0.065	1.52	0.030	0.039	0.029	–	–	–	–	–	4.32	($\gamma = 1.3$)
10.7	**2.13**	**0.06**	**1.52**	**0.032**	**0.040**	**0.051**	**0.16**	**0.065**	**0.37**	**2.5**	**0.010**	**1.33**	**1.30 A**
3.5	2.5	0.15	5.2	0.035	0.035	0.030	0.17	0.06	0.0	–	0.003	2.48	1.33 **B**
0.0	4.14	0.19	5.2	0.035	0.027	0.0	0.17	0.16	0.0	–	0.0	3.40	1.31 **K**

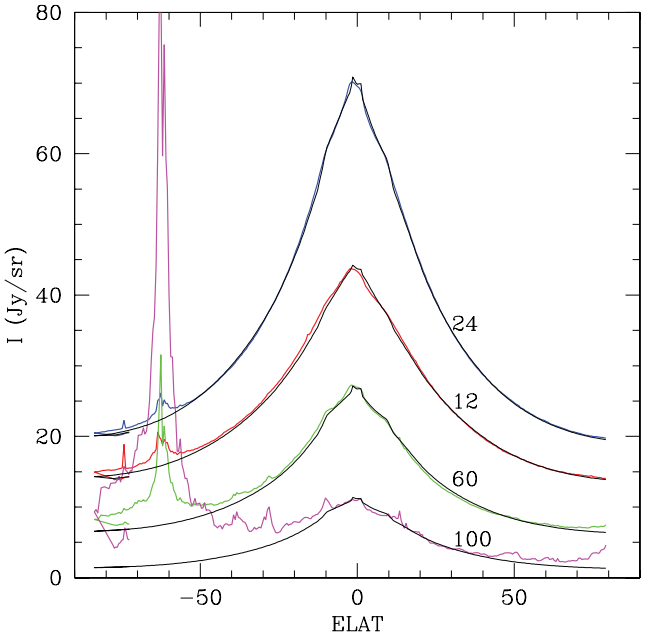

Figure 1. Comparison of *IRAS* scans at 12, 25, 60 and 100 μm with zodiacal dust model A. Scan is centred at solar longitude 90.°61.

forced on the solution). However, it is unclear how much of the interstellar dust within the Hoyle–Lyttleton column would make it into the fan. Much could simply be channelled on to the reverse side of the Sun. Note that at the ecliptic plane in model A, the interstellar dust contributes only 1 per cent of the zodiacal dust density at 1 au.

5 FITS TO DIRBE DATA

We used the DIRBE calibrated data files, which are given for each day of the mission. We first modelled the data for individual days using our best model A from table 2, excluding days where $\Sigma\mathrm{rms}^2 > 5(\mathrm{MJy\ sr}^{-1})^2$, which can arise for example because the Moon is in the field of view during the day. Data were used only if there were detections in all four bands at 12, 25, 60 and 100 μm, and only sky at $|b| > 40^\circ$ was used in the zodiacal modelling. We focused on three blocks of data where there were a significant number of contiguous days with good data, at day numbers 19–33, 51–95 and 216–264 in 1990. 40 of the 109 d in these three blocks were excluded. For a further 54 d analysed, distributed at random through the mission, none satisfied our constraint. The 69 d of data used in our solution covered 92 per cent of the sky, due to the particular scan strategy of *COBE*. After exclusion of $|b| < 40^\circ$ and areas affected by cirrus, we used 1.5 million observations in the solution, representing about 3 per cent of the total data. This is more than a factor of 20 times the amount of data used by Kelsall et al. (1998) in their solution

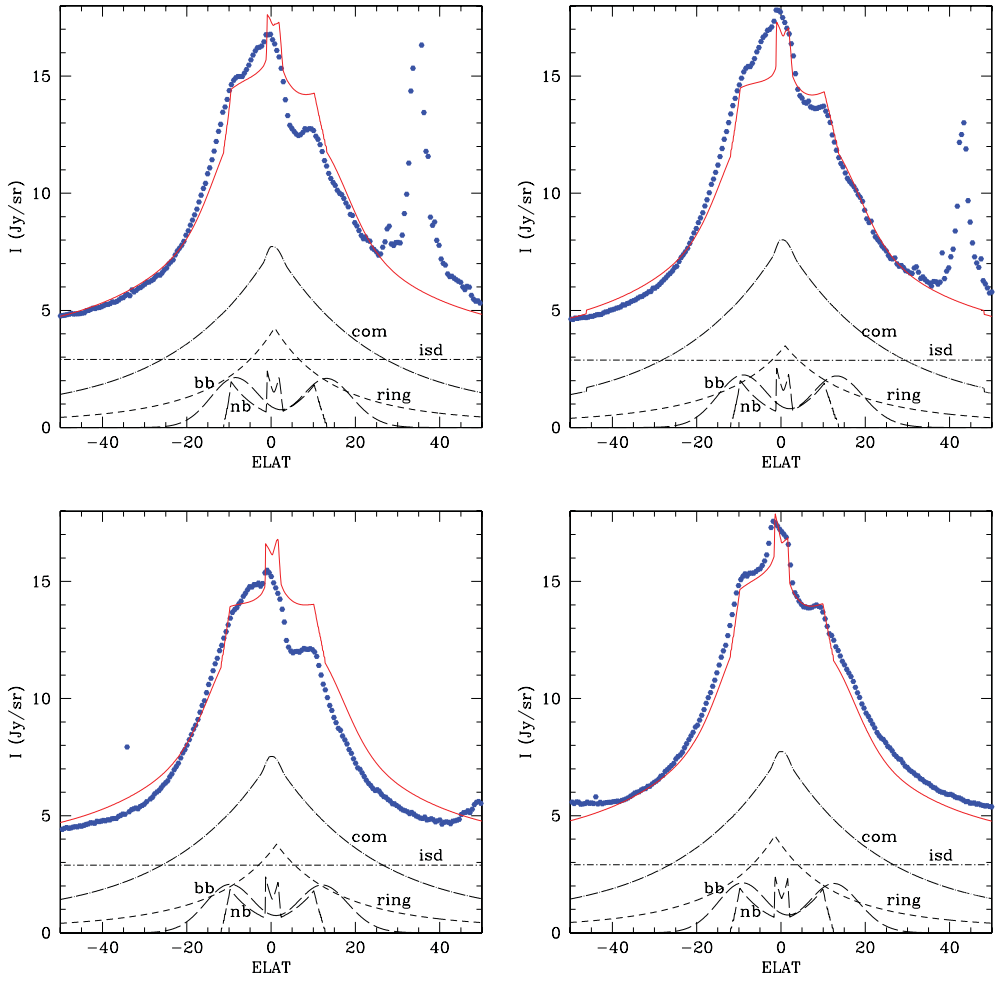

Figure 2. Comparison of *IRAS* scans at 25 μm, after subtraction of fan component (model A), with remaining components. Scans centred at (L to R) solar longitude 22.08, 33.40, 53.18 and 64.°93.

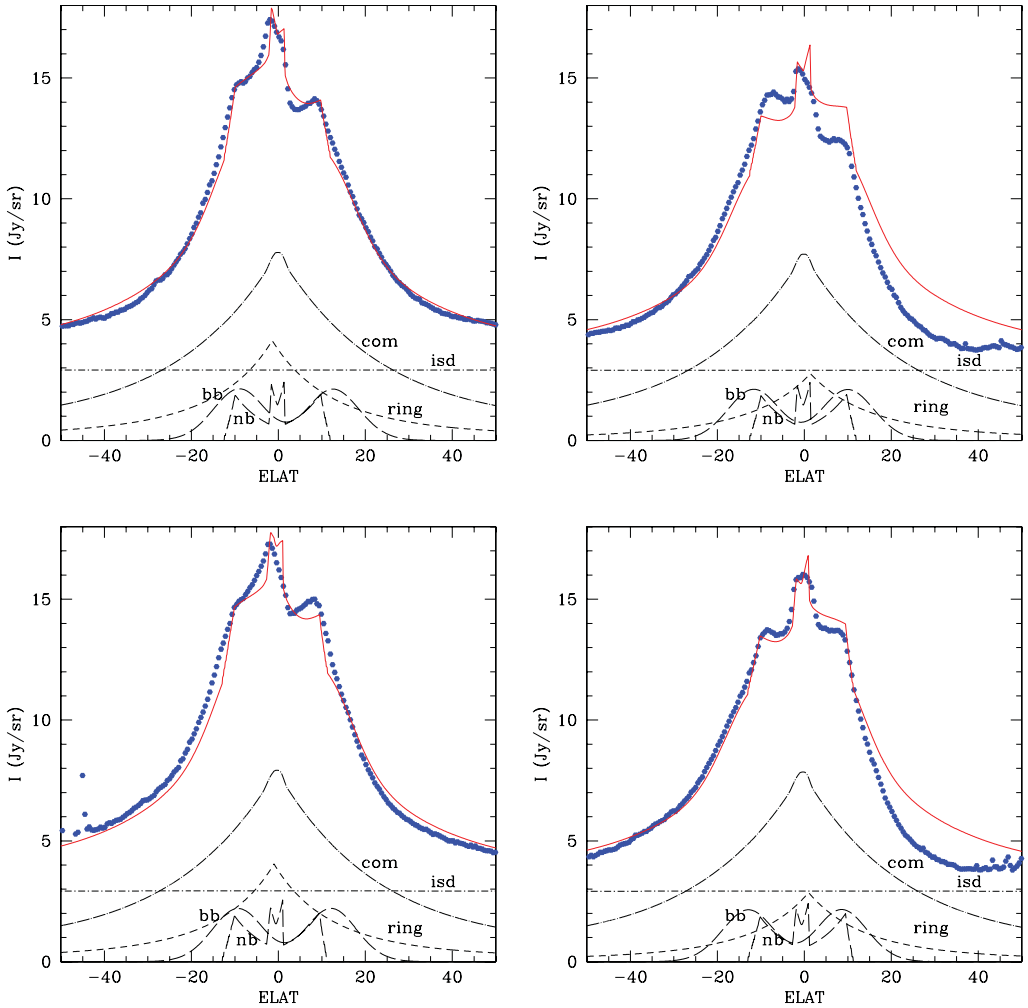

Figure 3. Comparison of *IRAS* scans at 25 μm, after subtraction of fan component (model A), with remaining components. Scans centred at (L to R) solar longitude 90.°61. 93.38, 121.°61 and 124.°99.

(0.13 per cent of the total data). We made no restriction on solar elongation angle.

We estimated the rms fluctuations for the DIRBE data at $|b| > 40^\circ$, $|\beta > 20^\circ$, after subtraction of the model A fan, as 0.80, 0.93, 0.67 and 0.80 MJy sr^{-1} at 12, 25, 60, 100 μm, and calculated χ^2 as above (last column in Table 1).

Fig. 4 shows fits with models A to data at solar elongation $90\pm1.^\circ0$, $|b| > 40^\circ$, on 1990 Jan 19. The nature of the *COBE* scan strategy do not allow pole-to-pole scans to be plotted, as for *IRAS*. We have shown fits to the 4.9 μm data, but have not used the latter in the parameter fits. The data at 140 and 240 μm were too noisy to plot, or to use in the solution. The model fits to the *COBE* data are excellent, and by excluding directions at $|b| < 40^\circ$ from the plots, we achieve much more compelling comparisons of the models with the DIRBE data than shown by Kelsall et al. (1998) (their fig 8). The combination of the larger beam of DIRBE, the precessing scan strategy of *COBE*, and the poorer signal-to-noise ratio compared with the *IRAS* scans, means that details of the asteroidal dust bands are much more poorly resolved by DIRBE. We were also unable to detect the trailing blob in the DIRBE data so the amplitude of this component could be determined only from *IRAS* data. Fig. 5 shows the corresponding plots for solar elongation 70 and $110 \pm 1.^\circ0$, illustrating that the model works well over a wide range of solar elongation.

We should check that the magnitude of our claimed isotropic interstellar dust component is not inconsistent with limits set in earlier studies. The magnitude of the isotropic component due to interstellar dust at 12, 25, 60 and 100 μm, respectively, are for model (A) 1.59, 2.90, 0.68, 0.23 MJy sr^{-1}. These are consistent with the limits on an isotropic background set by Hauser et al. (1998). Fig. 6, which shows χ^2_n as a function of the amplitude in the interstellar dust component, keeping the other parameters of model A fixed, illustrates the strong detection of the interstellar dust component in both *IRAS* and DIRBE data.

For model A, we investigated whether extending the broad-bands to 30 au (as proposed by Rowan-Robinson et al. 1991) affected the fit. We found no significant improvement in the χ^2_n for either the *IRAS* and DIRBE data. We also investigated whether making the broad-band dust grains smaller improved the fit, but again there was no improvement. However, the origin of this broad-band component does merit further study. It may arise from an older collision event between asteroid family members in the main belt. A much more distant origin in the Kuiper belt cannot be ruled out.

6 MODELS WITH FAN EXTENDED TO 5.2 au

Although the direct evidence from spacecraft data is consistent with the fan extending to $r = 1.53$ au, we have explored the possibility

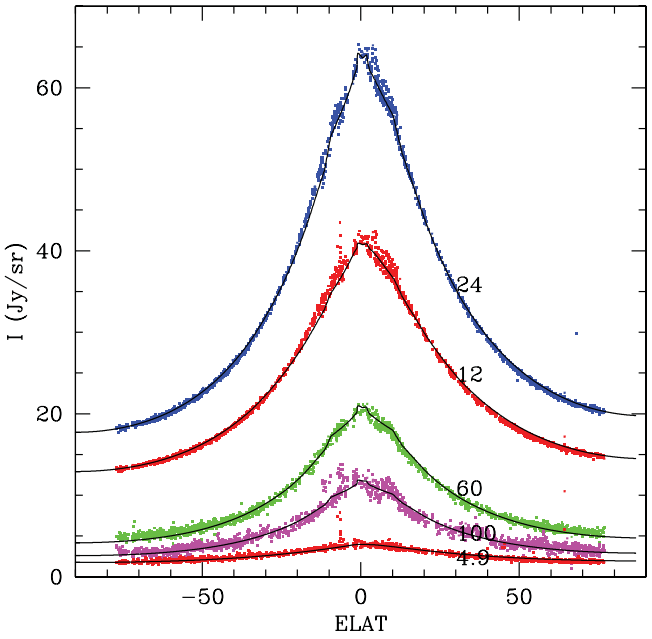

Figure 4. Comparison of DIRBE data at solar elongation 90 ± 1°0, from 2009 January 19, restricted to $|b| > 40°$, at 4.9, 12, 25, 60 and 100 μm, with model A.

that it could extend to the orbit of Jupiter at $r = 5.2$ au. We assume that 15 per cent of the zodiacal cloud interior to 1.53 au is supplied by the asteroidal bands, so that the amplitude of the extension from $r = 1.53$ to 5.2 au is at an amplitude 0.85 times that interior to 1.53 au. The main effect of such an extension is to increase the intensity at $|\beta| < 30°$. For our modified fan (equation 3) to remain consistent with observations it is necessary to change the parameters P, Q, but also to increase z_0. Line 5 of the table shows a fit with $Q = 3.5, P = 2.5$ and $z_0 = 0.15$ (model B, see Fig. 8). It was also necessary to reduce the amplitude of the outer narrow bands, AMP2 and of the broad-bands, AMPBB. The best combined fit to *IRAS* and DIRBE data has no cometary dust beyond 5.2 au, and the amplitude of interstellar dust is lower by a factor of 3 than in model A. The fits to the *IRAS* data are significantly worse than model A. Fig. 7 (L)

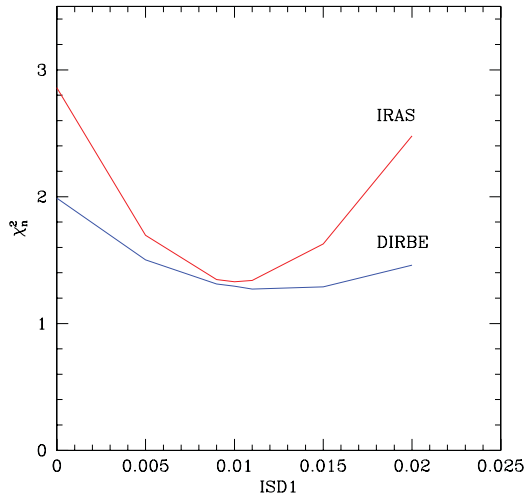

Figure 6. χ^2_n versus the interstellar dust amplitude, ISD1, for *IRAS* and DIRBE data.

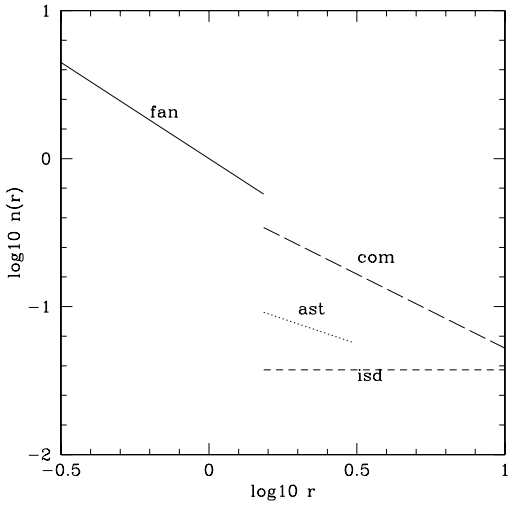

Figure 7. Dust density versus radius (au) for fan, cometary, asteroidal and interstellar dust in model A.

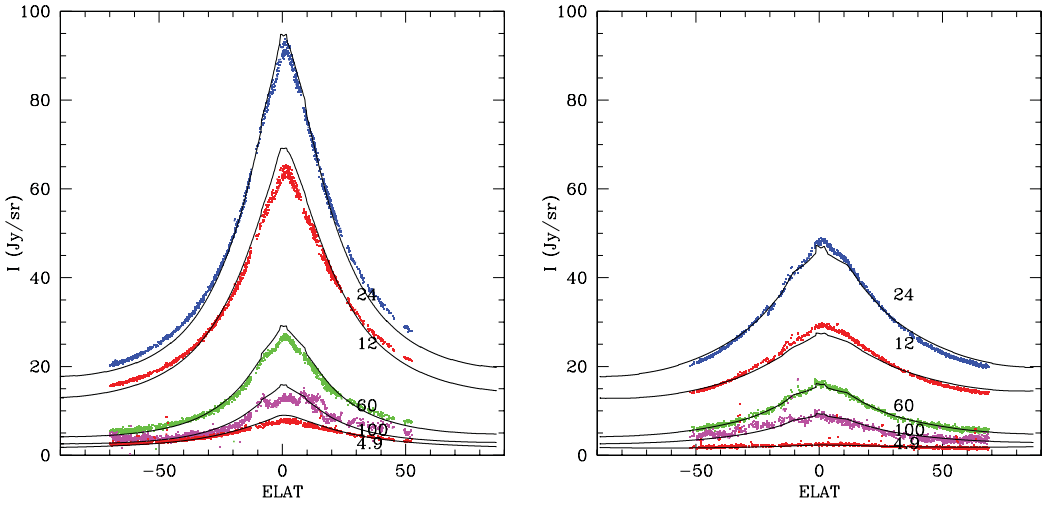

Figure 5. Comparison of DIRBE data at solar elongation 70 ± 1°0 (L) and 110±1°0 (R), from 2009 January 19, restricted to $|b| > 40°$, at 4.9, 12, 25, 60 and 100 μm, with model A.

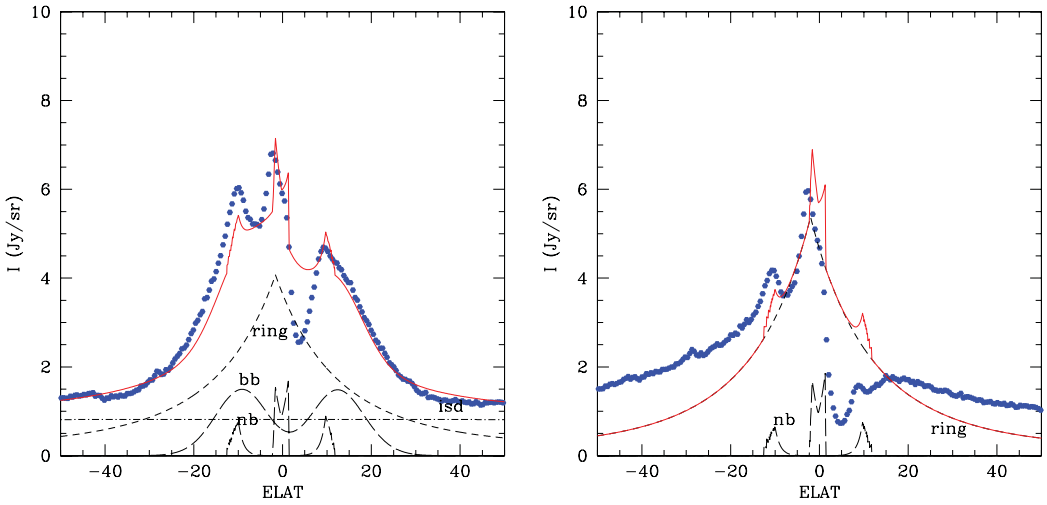

Figure 8. Comparison of *IRAS* scans at 25 μm, (L) after subtraction of fan component, extended to 5.2 au (model B), with remaining components; (B) after subtraction of Kelsall et al. (1998) fan (model K). Scans centred at solar longitude 90.°61.

shows the fit to the *IRAS* data at 25 μm after subtraction of the fan component.

We have also fitted the *IRAS* data with the Kelsall et al. (1998) fan model, plus ring and trailing blob. For the narrow bands we have simply used equation (4), with adjustments to the amplitudes and to G2 (=1.0). The Kelsall et al. fan changes shape at $\beta_0 \sim 10^\circ$ and thereby dispenses with the need for the broad-bands. The fit is noticeably worse for the *IRAS* data, with $\chi_n^2 = 3.40$ ($D_\nu = 0$). The extension of the fan to 5.2 au is not supported by the Divine (1993) analysis.

7 MASS–DENSITY IN ZODIACAL DUST

The parameter C_ν can be interpreted as $\pi a^2 Q_\nu n_0 a_0$, where a, Q_ν are the characteristic grain radius and absorption efficiency, n_0 is the grain number-density and $a_0 = 1$ au. Hence we can derive an order-of magnitude mass–density in grains, $\rho_{\rm gr} = n_0(4\pi a^3 \rho_0/3)$, where ρ_0 is the mean density of the grain, taken to be 2.5 gm cm^{-3}.

For model A, in the ecliptic plane at $r = 1.53$ au, and using C_ν at $\lambda = 12$ μm, we find

$\rho_{\rm gr}(Q_\nu/a(\mu{\rm m})) \sim 10^{-23.27}$ gm cm^{-3}, for the fan
$\sim 10^{-25.27}$ gm cm^{-3}, for the interstellar dust
$\sim 10^{-23.67}$ gm cm^{-3}, for the cometary dust.

For comparison Kimura et al. (2003) estimate the mass–density of interstellar dust at $r = 1.5$ au as $10^{-25.3 \pm 0.7}$ gm cm^{-3}, so our value is consistent with this for a ∼2−4μm, $Q_\nu \sim 1$. On the other hand they estimate the mass–density of interstellar dust at $r > 4$ au as $10^{-26.43(+0.26,\ -0.60)}$ gm cm^{-3}, attributing the difference to gravitational focusing of the dust in the inner Solar system. Our assumed isotropic uniform dust density is therefore an order of magnitude higher than that measured by Ulysses at $r > 4$ au. Further work will be needed to assess whether the density of interstellar grains has a strong dependence on radial distance. Our dust density estimates are approximate, but the satellite estimates are also indirect, based on the measured charge.

8 DISCUSSION

Our model provides fits to the *IRAS* and DIRBE data significantly better than those achieved in the previous analyses and shows good consistency with the major components identified by Divine (1993) in the Ulysses spacecraft data. The major new constituents compared to JRR are the interstellar and cometary components, corresponding to the 'halo' component of Divine (1993).

In model A, the relative contributions of cometary, interstellar and asteroidal dust to the density of the fan at 1.5 au are 70.4, 7.5 and 22.2 per cent, and the density of the fan is exactly accounted for by these components. This is the first analytical fit to the zodiacal infrared data in which the origin of the fan is fully accounted for. Our assumed isotropic uniform density of interstellar grains is consistent with values measured by Ulysses at 1.5 au, but an order of magnitude higher than values measured at $r > 4$ au. Further work will be needed to assess whether the density of interstellar grains has a strong dependence on radial distance, as proposed by Kimaru et al. (2003).

Our approach gives a valid independent perspective on dust in the Solar system to that given by dynamical simulation of the different components (e.g. Gustafsen et al. 1987; Durda et al. 1997; Dikarev et al. 2005; Ipatov et al. 2008; Nesvorny et al. 2010). Although predictions of dynamical models with just asteroidal and cometary dust have been compared with *IRAS* (Nesvorny et al. 2010) and *COBE* (Dikarev et al. 2005) data, we find that to fit both sets of data to the accuracy achieved here requires the additional ingredient of a homogenous, isotropic component, corresponding to interstellar dust.

While cometary and asteroidal dust spiral inwards very slowly and can experience strong orbital changes at the crossing of planetary orbits, the fast-moving interstellar dust is almost unaffected by the planets and is trapped in the inner Solar system by the sun's gravity through Hoyle–Lyttleton accretion. The smallest grains will also be repelled from a cylindrical column behind the Sun by radiation pressure and magnetic forces. This column would also show a concentration of larger grains being accreted towards the Sun. Unfortunately the direction of this column [$(\lambda, \beta) \sim (-172^\circ, -5^\circ)$; Kimaru et al. (2003)] is rather close to the ecliptic plane, so it cannot be resolved in maps of the *IRAS* background emission. Detection of the downstream accretion column would be an important confirmation of the interstellar dust component.

Nesvorny et al. (2010) carried out an interesting simulation of the dynamics of cometary dust in the Solar system. Their estimate that cometary dust provides over 90 per cent of the zodiacal dust in the

inner Solar system is higher than our model predicts. We estimate that cometary dust could contribute 60–80 per cent, with asteroidal and interstellar dust contributing 20–40 per cent between them. Our estimate of the relative proportions of cometary and asteroidal dust agree well with the estimate of Liou et al. (1995) from a dynamical model.

We find that the contribution of interstellar dust may be more significant than estimated by Grogan et al. (1996). The DIRBE data iare crucial here in demonstrating the presence of an isotropic foreground component at 12, 25, 60 and 100 μm. The amplitude of this foreground does not conflict with the isotropic background limits set by Hauser et al. (1998).

We find strong support for the Hicks et al. (1974) proposal, extended by May (2007), based on kinematical observations, that interstellar dust is a significant contributor to the local zodiacal dust cloud, although the density we find in the ecliptic plane is much lower than that estimated by May. There is a need for a new ground-based kinematic study of zodiacal dust, ideally extended over several years to test for time variation through the solar cycle. The models presented here can also be tested by dynamical simulations and by further in situ measurements from spacecraft at $r > 5$ au.

The zodiacal dust cloud appears to be supplied by a combination of cometary dust, dust from collisions between members of asteroid families in the asteroid belt, and interstellar dust. It therefore carries detailed information about the recent history of the Sun's debris disc and merits far more intensive study than it has received to date.

REFERENCES

Altobelli N., Kempf S., Landgraf M., Srama R., Dikarev V., Kruger H., Moragas-Klostermeyer G., Grun E., 2003, J. Geophys. Res., 108, 8032

Dermott S. F., Nicholson P. D., Burns J. A., Houck J. R., 1984, Nat, 312, 505

Dermott S. F., Jayaraman S., Xu X. L., Gustafson B. A. S., Liou J. C., 1994, Nat, 369, 719

Deul E. R., Wostencroft R. D., 1988, A&A, 196, 277

Dikarev V., Grun E., Baggaley J., Galligan D., Landgraf M., Jehn R., 2005, Adv. Space Res., 35, 1282

Divine N., 1993, J. Geophys. Res., 98, 17029

Durda D. D., Dermott S. F., 1997, Icarus, 130, 140

East I. R., Reay N. K., 1984, A&A, 139, 512

Giese R. H., Kinateder G., Kneissel B., Rittich U., 1985, in Giese R. H., Lamy P., eds, Properties and Interactions of Interplanetary Dust. Reidel, Dordrecht, p. 225

Giese R. H., Kneissel B., Rittich U., 1986, Icarus, 68, 395

Grogan K., Dermott S. F., Gustafson B. A. S., 1996, ApJ, 472, 812

Grogan K., Dermott S. F., Xu Y. L., 2001, Icarus, 152, 251

Grun E. et al., 1993, Nat, 362, 428

Grun E., Srama A., Kruger H., Kempf S., Dikarev V., Helfert S., Moragas-Klostermeyer G., 2005, Icarus, 174, 1

Gustafsen B. A. S., Misconi N. Y., Rusk E. T., 1987, Icarus, 72, 568

Hauser M. et al., 1998, ApJ, 508, 25

Hicks T. R., May B. H., Reay N. K., 1972, Nat, 240, 401

Hicks T. R., May B. H., Reay N. K., 1974, MNRAS, 166, 439

Hoyle F., Lyttleton R. A., 1939, Proc. Cambridge Philos. Soc., 35, 405

Ipatov S. I., Kutyrev A. S., Madsen G. J., Mather J. C., Moseley S. H., Reynolds R. J., 2006, 37th Annual Lunar and Planetary Science Conference, League City, Texas

Ipatov S. I., Kutyrev A. S., Madsen G. J., Mather J. G., Moseley S. H., Reynolds R. J., 2008, Icarus, 194, 769

Jones M. H., Rowan-Robinson M., 1993, MNRAS, 264, 237

Kelsall T. et al., 1998, ApJ, 508, 44

Kimura H., Mann I., Jessberger E. K., 2003, ApJ, 582, 846

Kruger H. et al., 2010, Planet. Space Sci., 58, 951

Leinert C., 1985, in Giese R. H., Lamy P., eds, Properties and Interactions of Interplanetary Dust. Reidel, Dordrecht, p. 369

Leisawitz D. et al., 1994, BAAS, 26, 1409

Liou J. C., Dermott S. F., Xu Y. L., 1995, Planet. Space Sci., 43, 717

Low F. J. et al., 1984, ApJL, 278, L19

Madsen G. J., Reynolds R. J., Ipatov S. I., Kutryev A. S., Mather J. C., Moseley S. H., 2006, in Dust in Planetary Systems. Kaua'i, Hawaii, LPI Contribution No. 1280, p. 111

Mann I., 2010, ARA&A, 48, 173

May B. H., 2007, PhD thesis, Imperial College

Murdock T. L., Price S. D., 1985, AJ, 90, 375

Nesvorny D., Jenniskens P., Levison H. F., Bottke W. F., Vokrouhlicky D., Gounelle M., 2010, ApJ, 713, 816

Reach W. T. et al., 1995, Nat, 374, 521

Reay N. K., Ring J., 1968, Nat, 219, 710

Reynolds R. J., Madsen G. J., Moseley S. H., 2004, ApJ, 612, 1206

Rowan-Robinson M., Hughes J., Vedi K., Walker D. W., 1990, MNRAS, 246, 273

Rowan-Robinson M., Hughes J., Jones M., Leech K., Vedi K., Walker D. W., 1991, MNRAS, 249, 729

Sterken V. J., Westphal A. J., Altobelli N., Postberg F., Srama R., Grun E., 2012a, 43rd Lunar and Planetary Science Conference, League City, Texas

Sterken V. J., Altobelli N., Kempf S., Schwehm G., Srama R., Grun E., 2012b, A&A, 538, A102

Sykes M. V., 1990, Icarus, 84, 267

Sykes M. V., Greenberg R., 1986, Icarus, 65, 51

Sykes M. V., Lebofsky L. A., Hunten D. M., Low F., 1986, Sci, 232, 1115

This paper has been typeset from a TEX/LATEX file prepared by the author.